Supplemental Figure Legends

Table S1. Microarray Data, Related to Figure 1

List of genes found to be differentially expressed in the microarray. Each tab contains a separate list: those genes found to be upregulated or downregulated in *apterous* or *slouch* expressing cells compared to *twip-actin-GFP*.

Table S2. Quantification of *in situ* Hybridization Analysis, Related to Figure 1

in situ hybridizations were scored without knowledge of the probe for either mesodermal or ubiquitous expression at each of the three stages. For some probes, expression was ubiquitous at one stage, but mesodermal at a different stage.

Table S3. Comparison of Microarray Data to other Data Sets, Related to Figure 1

Comparison of microarray data to that found in other studies: Schnorrer et al., 2010, Artero et al., 2003, Estrada et al., 2006 and Tomancak et al., 2002.

Figure S1. mRNA Expression of Genes Identified in the Microarray, Related to Table 1

Lateral views (20X) of stage 10-11 (left), stage 12-13 (middle) and stage 15-16 (right) *wild-type* (OreR) embryos that have been hybridized against the indicated *in situ* probes (far right). Mesodermal staining was detected in at least one of the three stage categories for each of the genes that, when mutated, display muscle defects. Arrows (blue) point to a representative example of mesodermal expression at each stage: for stage 10-11, somatic mesoderm expression of *Gug;* for stage 12-13, FC expression of *chn*; and for stage 15-16, ventral muscle expression of *Elo-B*. Images were captured using an Axiocam digital camera (Zeiss).

Figure S2. Phenotypes of Homozygous Mutant Alleles, Related to Figure 2

(A) Diagram of wild-type muscle pattern of three hemisegments at stage 16. The LT muscles are green and the VA muscles are magenta (B-M) Stage 16 embryos stained with anti-Myosin heavy chain (MHC). In this and all following figures, unless indicated, approximately 3 hemisegments are shown, Scale bar, 25 μm. Mutant phenotypes are indicated by filled arrows (misshapen), open arrows (missing muscles), line arrows (extra muscles), filled arrowheads (misattached muscles) and open arrowheads (unattached myospheres). (N) Percentage of hemisegments (blue) and embryos (orange) displaying aberrant phenotypes in each mutant background. Five abdominal hemisegments from at least 20 embryos for each genotype were quantified.

Figure S3. Cuticle Phenotypes of Mutant Alleles, Related to Figure 2

Lateral dark field views (20X) of stage 17 embryos of the indicated genotypes to show their cuticle patterns. Images were captured using an Axiocam digital camera (Zeiss).

Figure S4. Expression of Newly Identified Factors in Muscle Founder Cells, Related to Figure 2

Lateral views (63X) of stage 13 *wild-type* (OreR) embryos stained to show expression in the muscle. For Sin3A, Skd, Crp, Chn and Alh, embryos expressing the *rp298-lacZ* transgene in muscle FCs were stained with anti-β-galactosidase (left, single channel, white and right, merge, green) and the indicated antibodies (center, single channel, white and right, merge, magenta) to show co-expression in muscle founder cells (arrows, blue). For Elo-B, OreR embryos were stained with anti-MHC (left, single channel, white and right, merge, green) and human anti-Elo-B (center, single channel, white and right, merge, magenta) to show co-expression in the muscle.

Figure S5. *Sin3A08269* Mutants have Muscle Defects and Changes in Integrin Levels, Related to Figure 3 (A-B') Stage 16 embryos stained for MHC *(left)* or the *Drosophila* beta PS

Integrin Mys *(right).* 3 hemisegments shown. Yellow arrows point towards laterally oriented muscles, while blue arrows point to the segment border. White arrows point to the absence of Integrin accumulation at the dorsal and ventral poles of the LT muscles. (C) Quantitative PCR analysis of alpha PS Integrin (*mew*) and beta PS Integrin (*mys*) mRNA levels in wild-type (orange) and *Sin3A* mutant embryos (blue). Reduction of *mew* and *mys* expression is statistically significant.

Figure S6. Sin3A Acts as a Buffering Factor in *Drosophila* Embryonic Muscle, Related to Figure 5

(A) Quantification of *Slou* expression by RT-PCR in *wild-type* (OreR) and *Sin3A08269* homozygous embryos at the indicated stages. (B-C) Stage 16 embryos of the indicated genotypes stained with antibody against MHC. Approximately three hemisegments are shown. Arrows point to the wild-type number of 4 LT muscles (B) and the increased number of LTs in *Sin3A08269/+; DMef2-Gal4 > UAS-Ara* embryos. (D-E) Stage 16 embryos of the indicated genotypes stained with antibody against MHC. Approximately three hemisegments are shown.

Dobi et al. Supplemental Table 2

	Stage 10-11	Stage 12-13	Stage 15-16	Any Stage
mesodermal expression	69%	49%	39%	80%
ubiquitous expression	11%	11%	11%	23%

Dobi et al.,
Figure S1

Stage 10-11

Stage 12-13

Stage 15-16

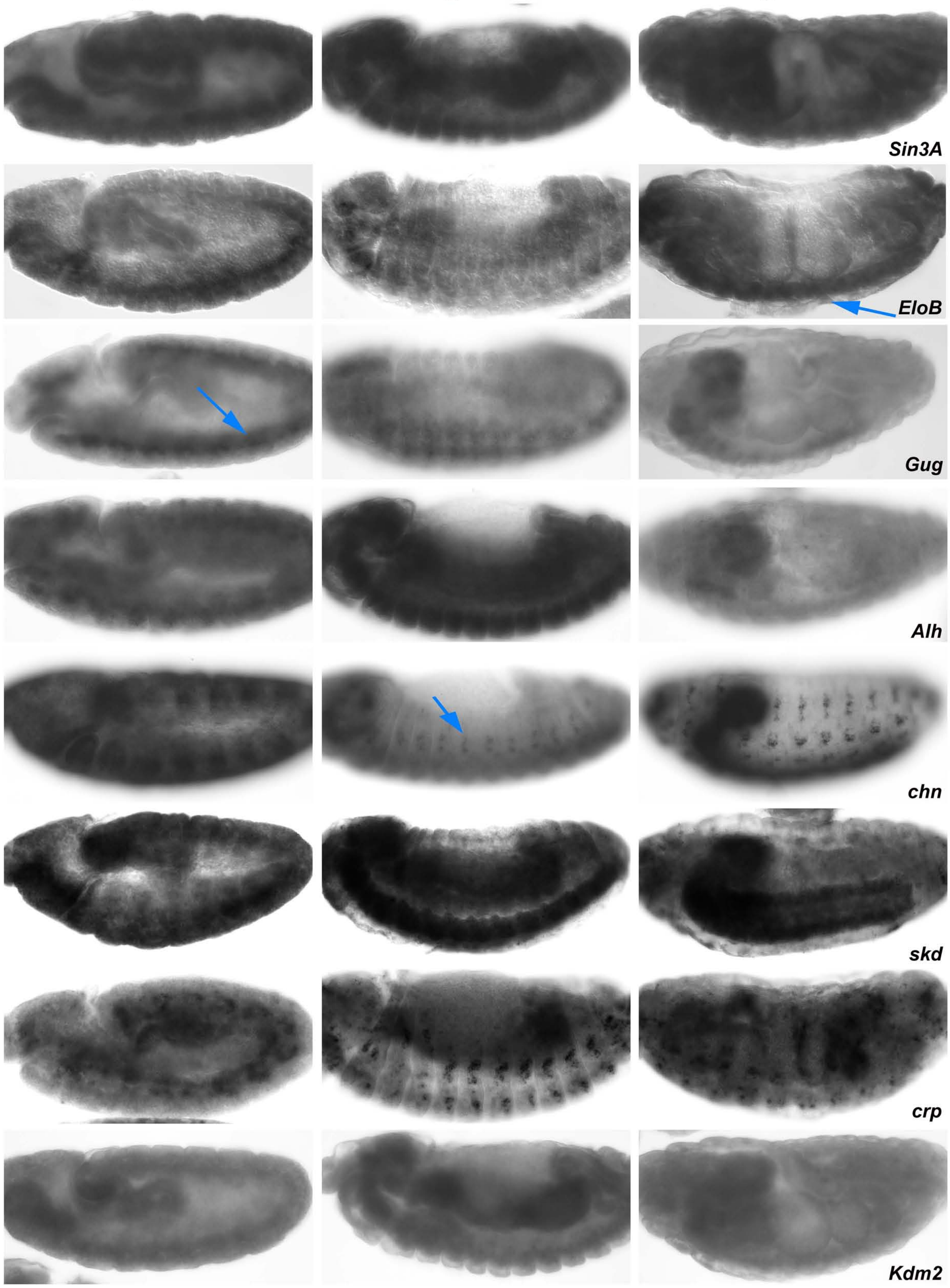

Dobi et al.
Figure S2

A

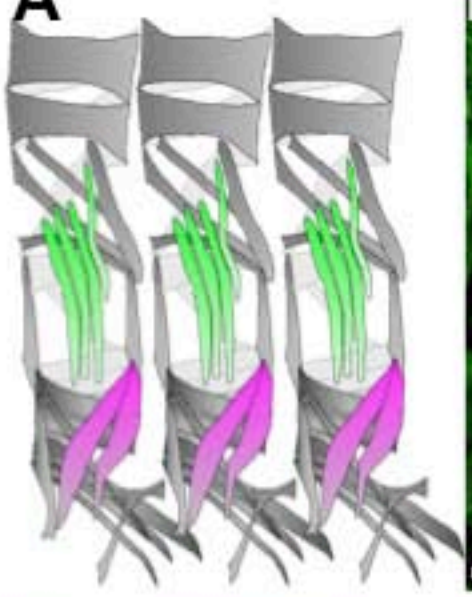

B

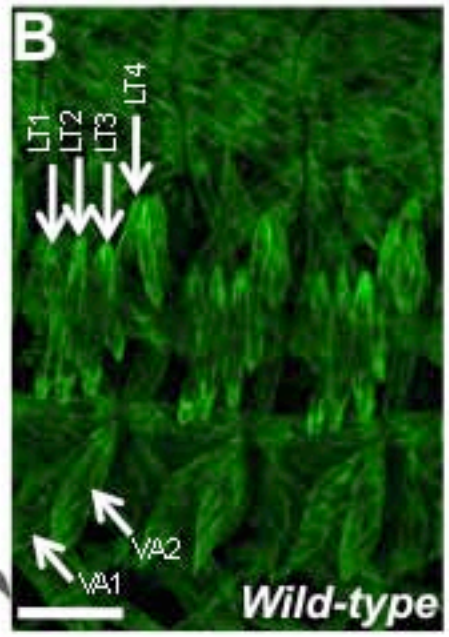

C

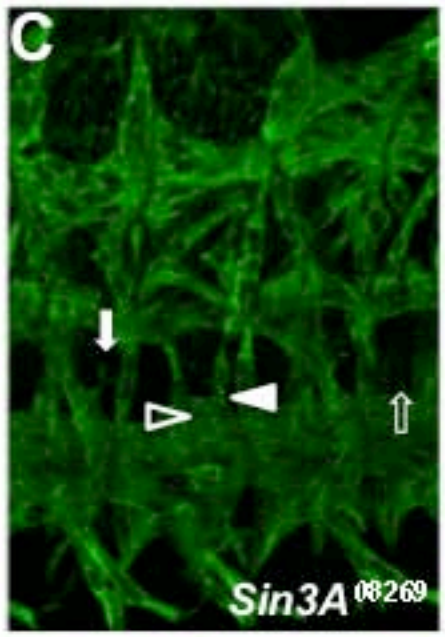

D

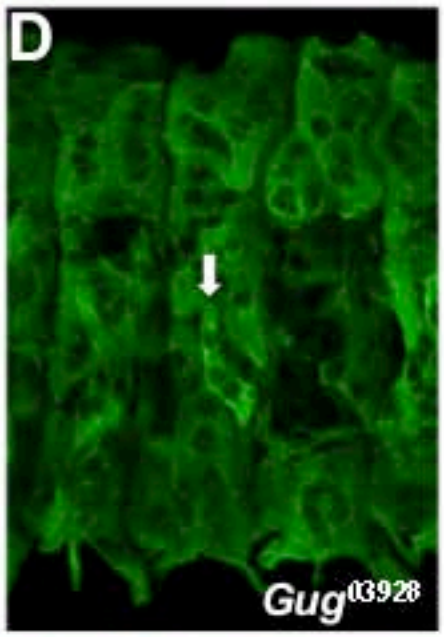

E

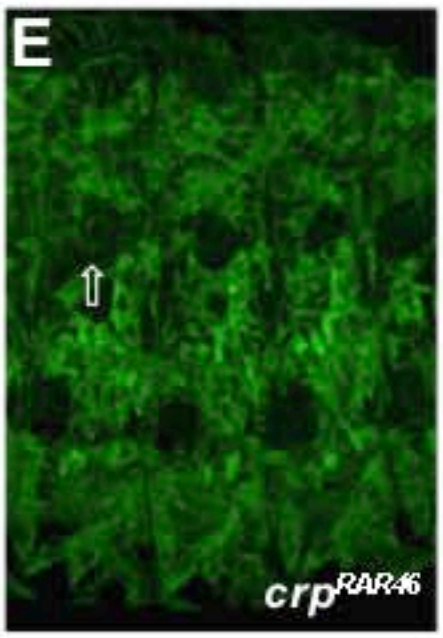

F

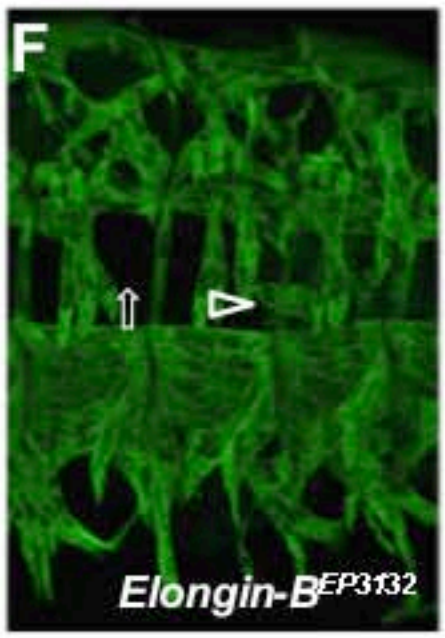

G

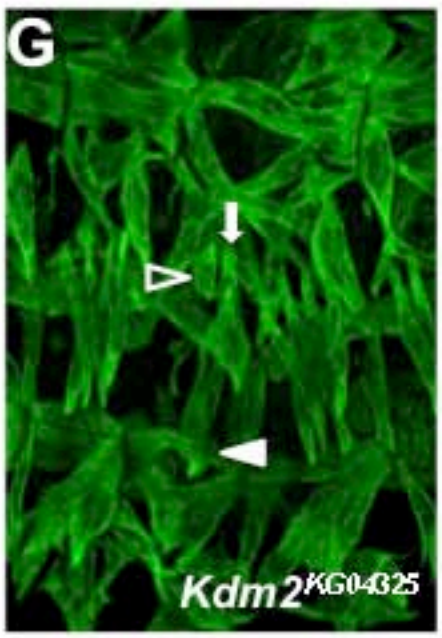

H

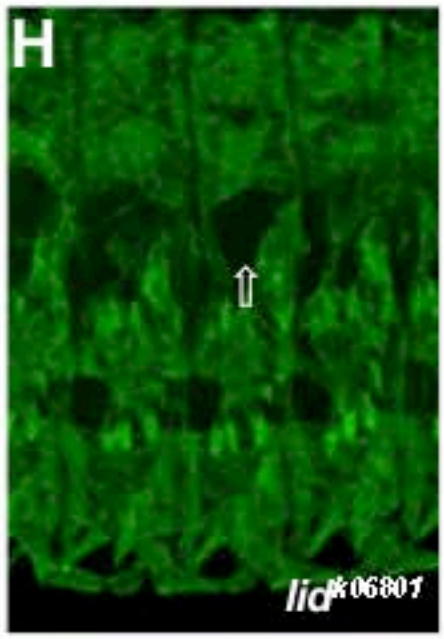

I

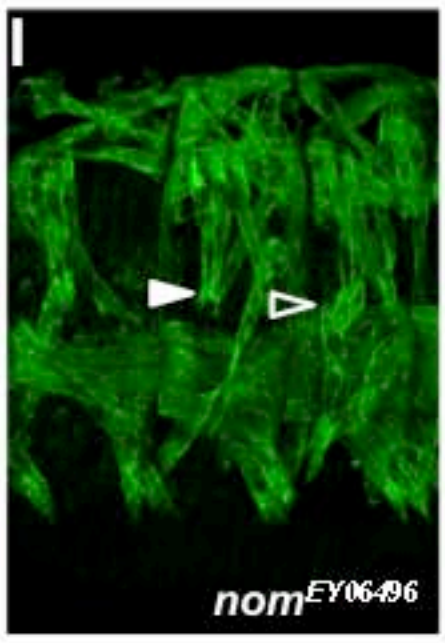

J

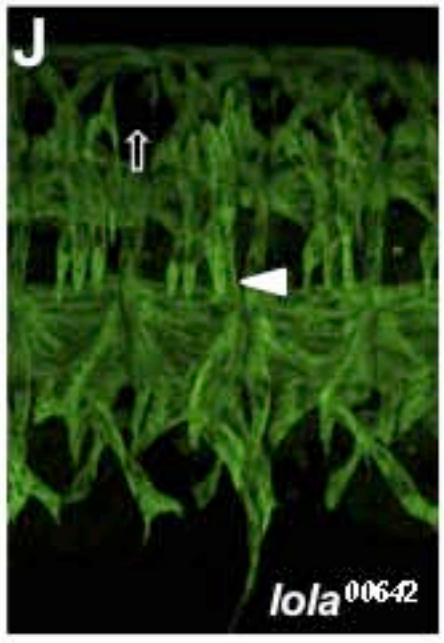

K

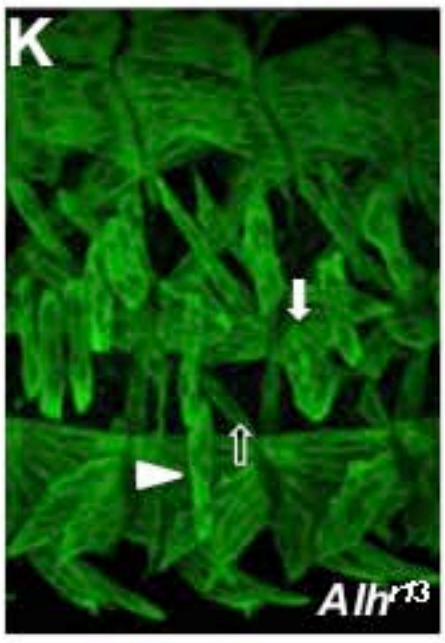

L

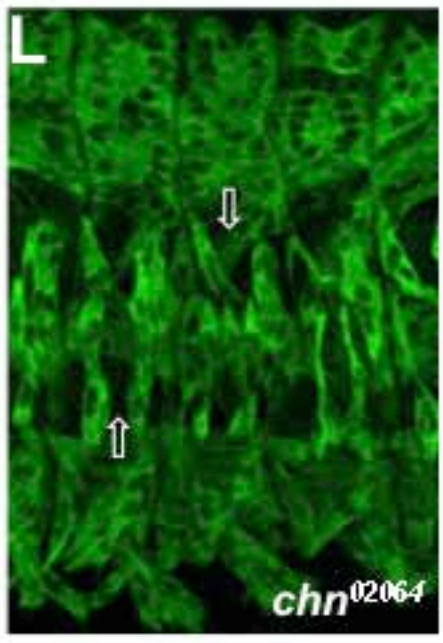

M

N

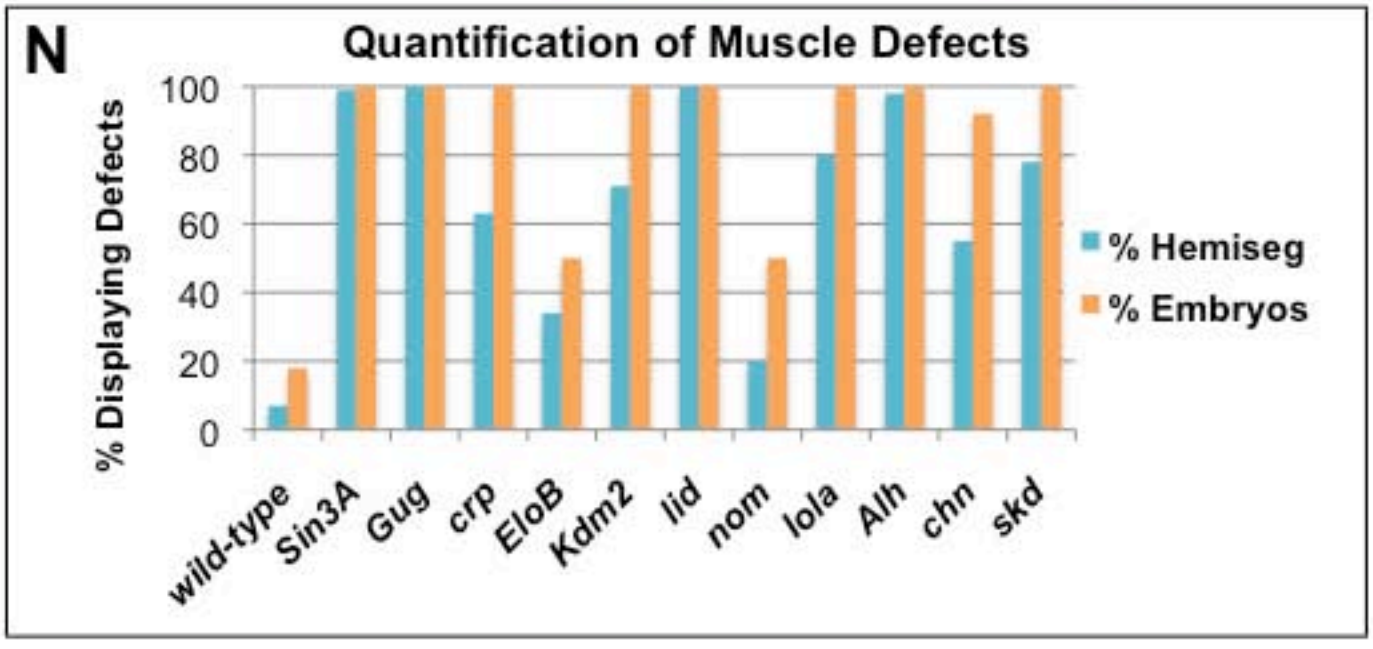

Dobi et al., Figure S3

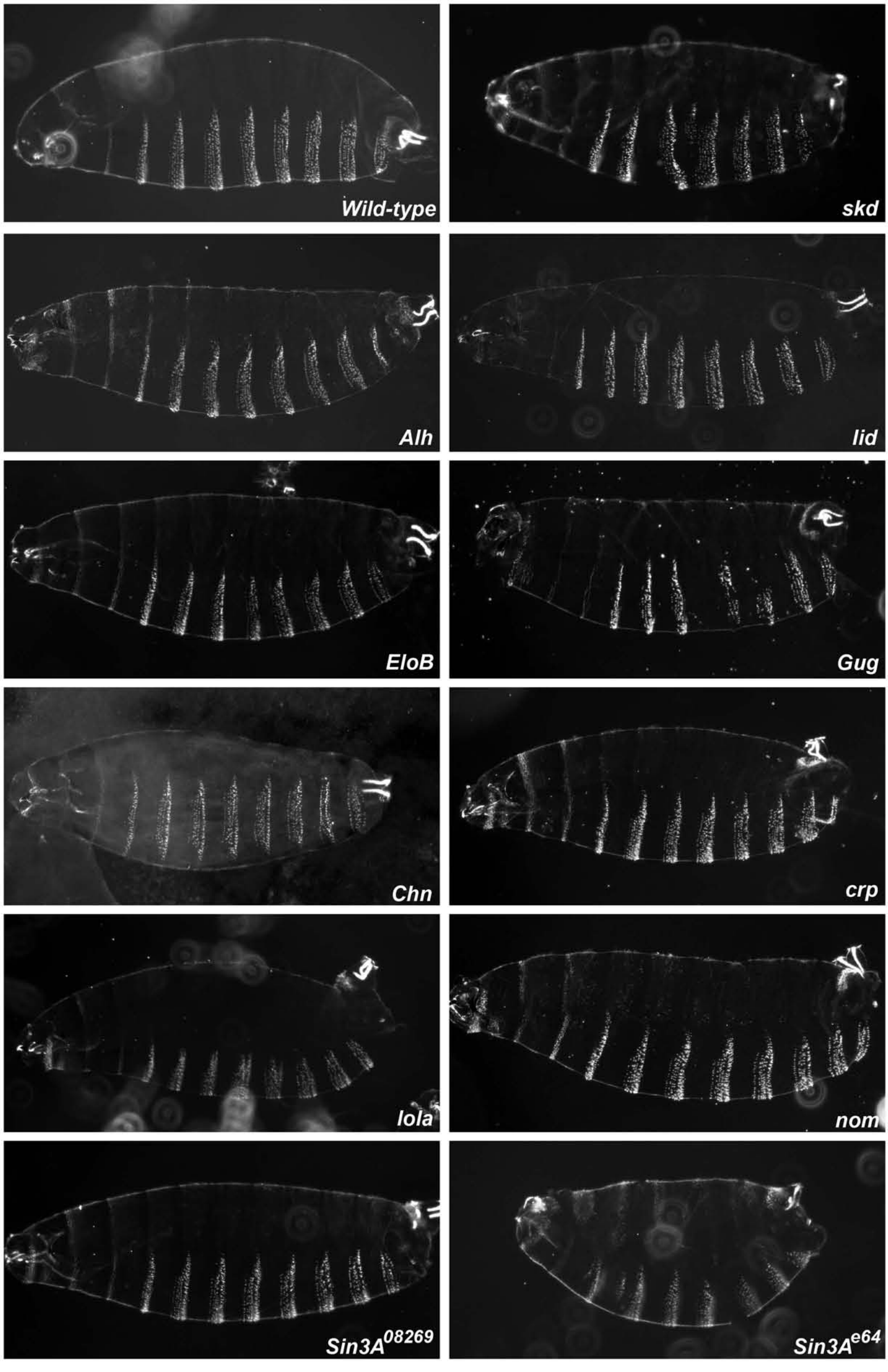

Dobi et al., Figure S4

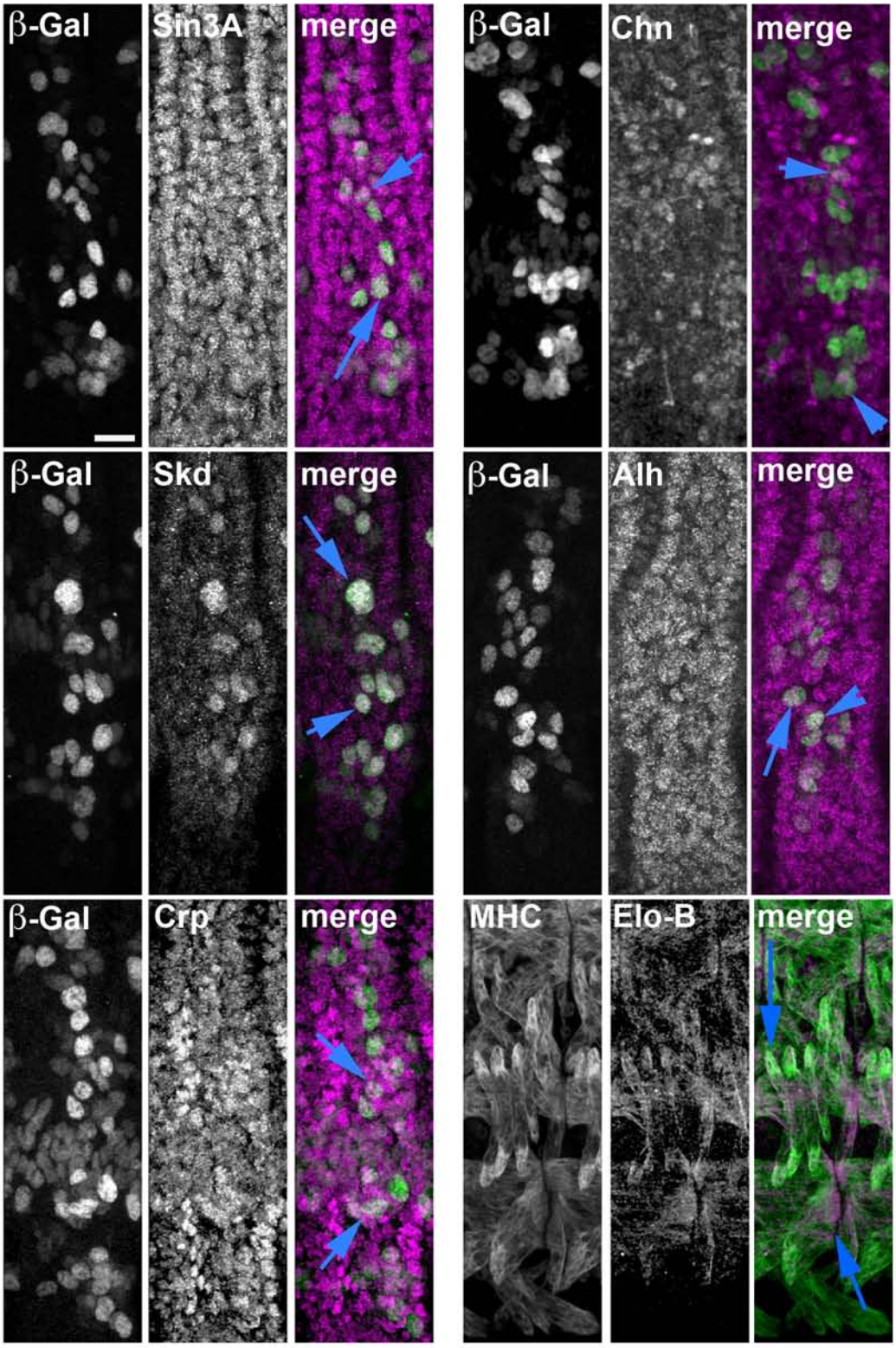

Dobi et al.,
Figure S5

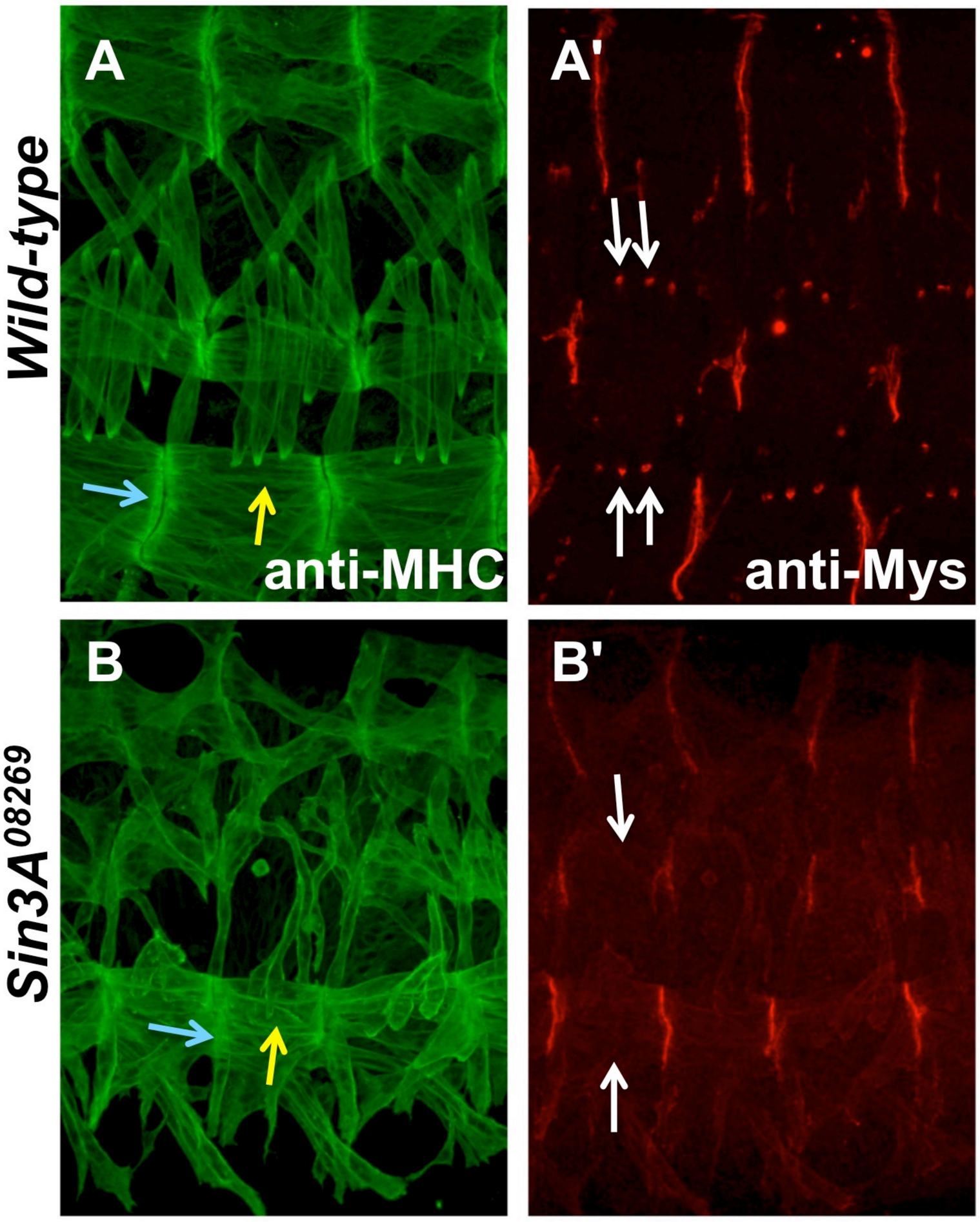

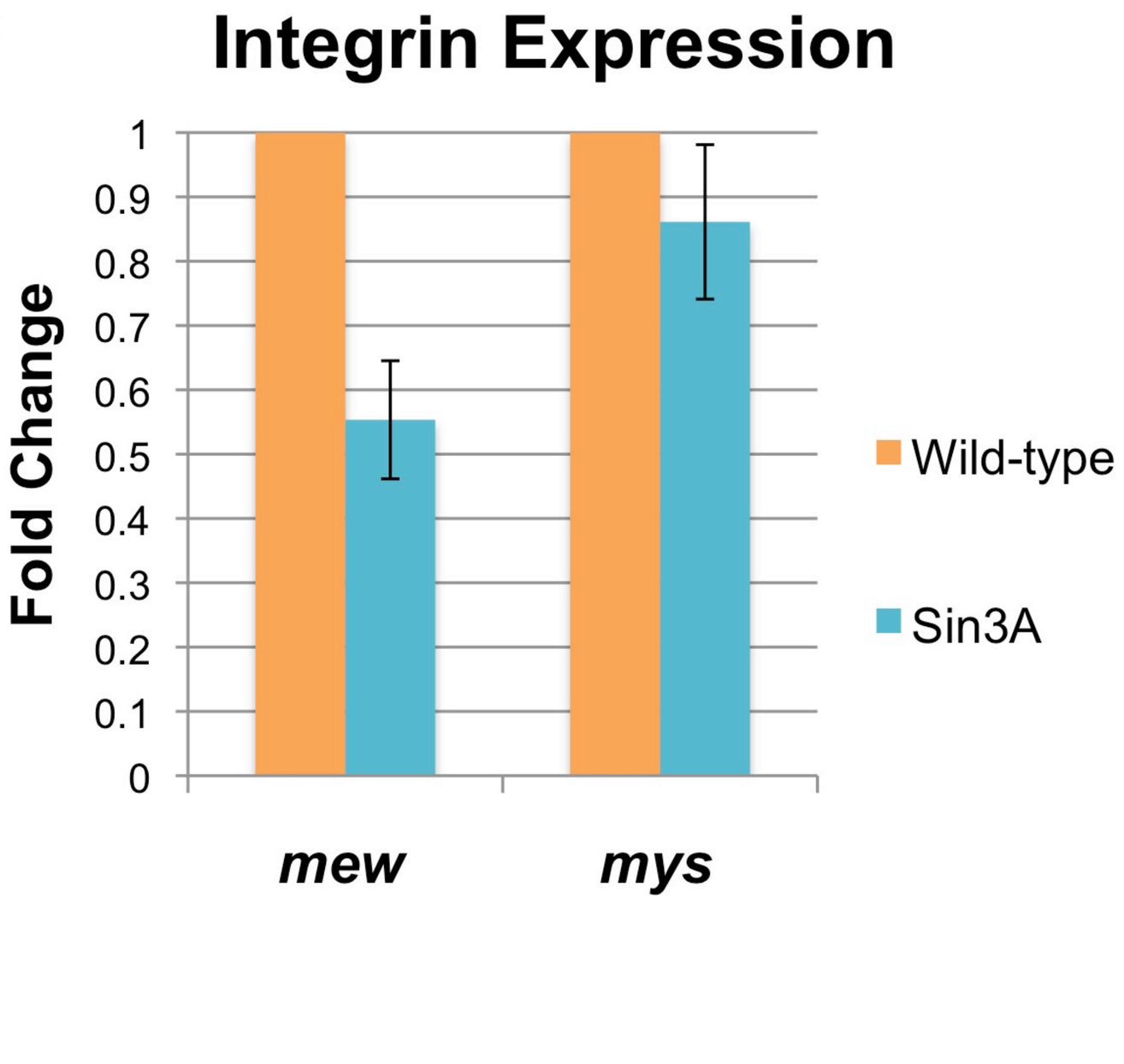

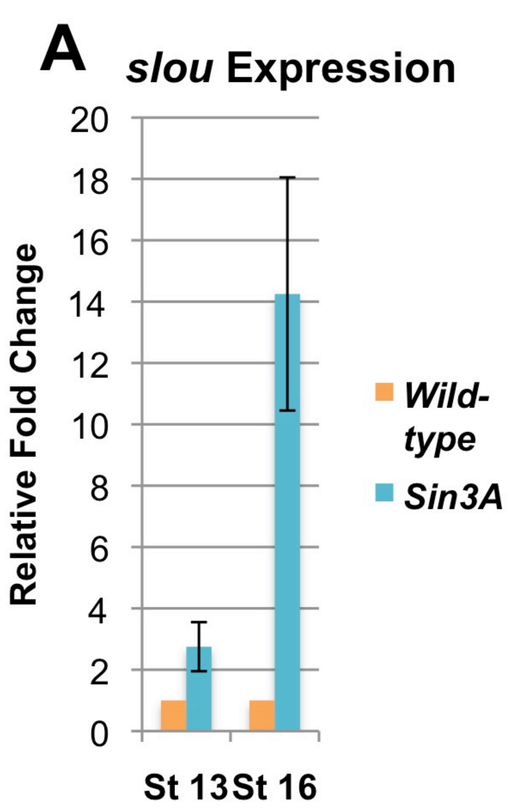

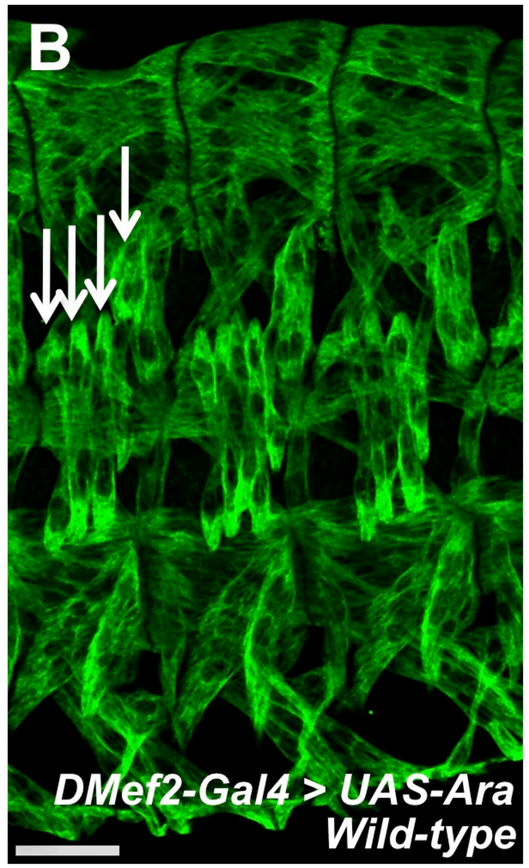

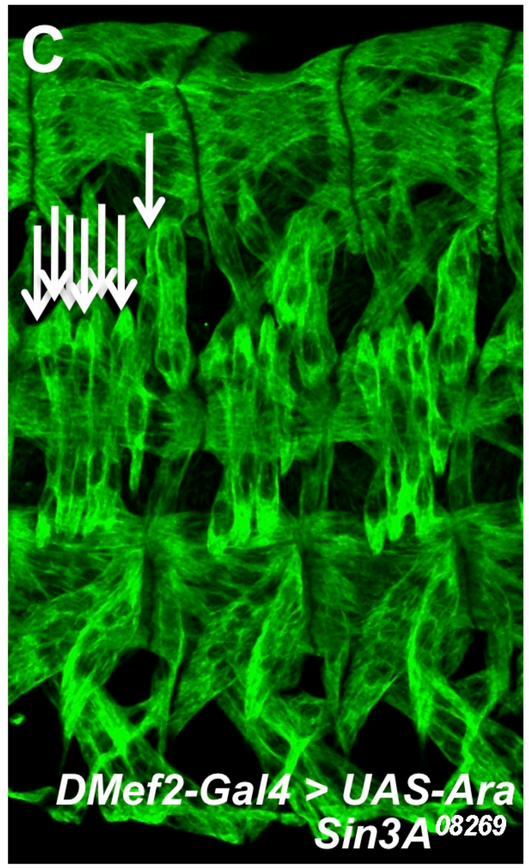

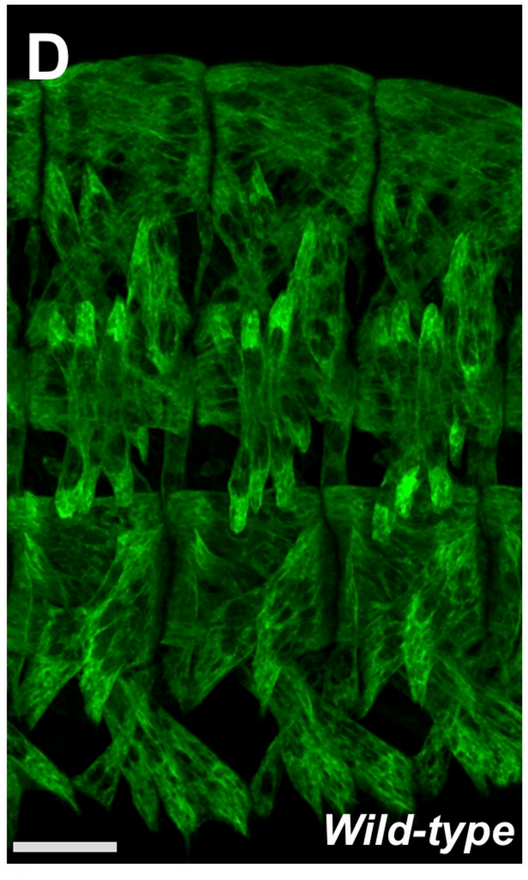

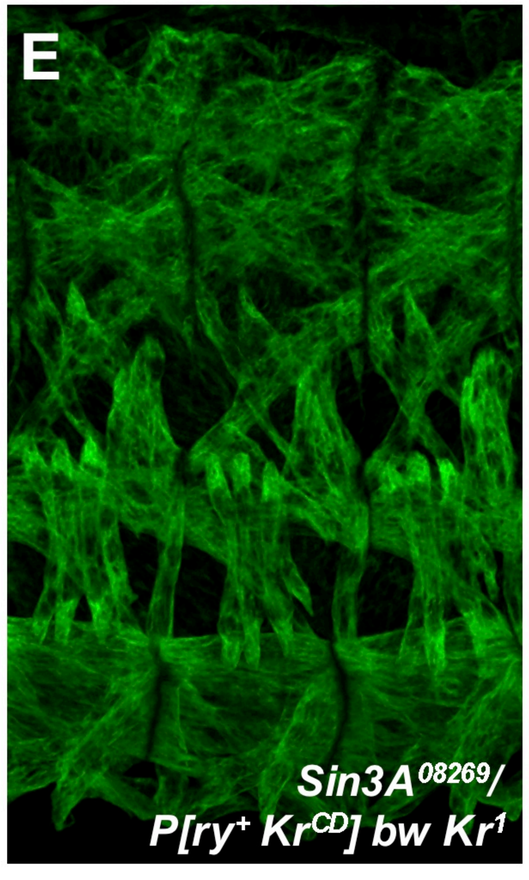

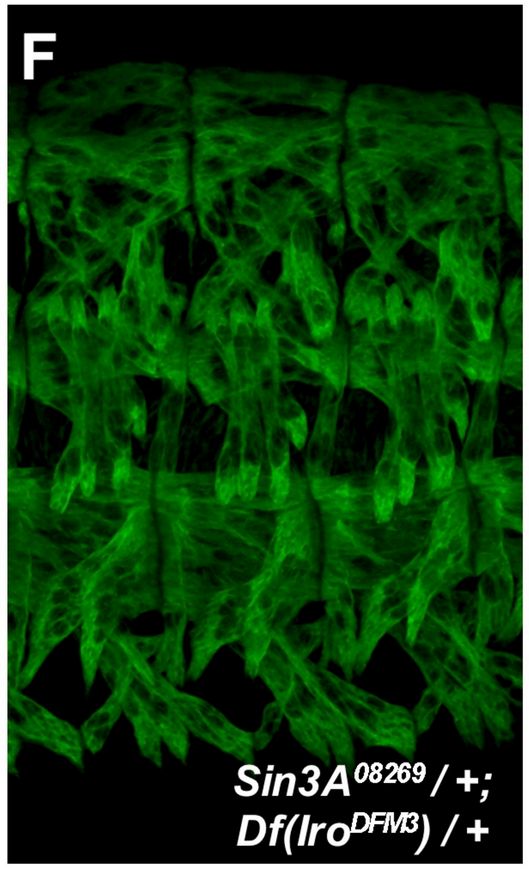

Dobi et al.,
Figure S6

SUPPLEMENTAL EXPERIMENTAL PROCEDURES

Fly Stocks Used in This Study

Fly stocks used were: *apterous$_{ME}$-GFP* (Richardson et al., 2007), *slouch$_{ME}$-RFP* (Schnorrer et al., 2007) *twi$_{promoter}$-actin-GFP* (Richardson et al., 2007), *apterous$_{ME}$-NLS::dsRed* (Metzger et al., 2012), *twi-Gal4;24B-Gal4* (Baylies and Bate, 1996), *UAS-Kr; UAS-Kr* (Ruiz-Gómez et al., 1997), *P[ry^{+} Kr^{CD}]bw Kr^{1}* (Ruiz-Gómez et al., 1997); *UAS-ara* (Carrasco-Rando et al., 2011); *Df(3L)iro^{DFM3}* (Gomez-Skarmeta et al., 1996); *rp298-lacZ* (Nose et al., 1998); *DMef2-Gal4* (Halfon et al., 2000), *Sin3A^{08269}* (Neufeld et al., 1998), *Sin3A^{e64}* (Neufeld et al., 1998) , *Sin3A^{EP2387}* (Burgio et al., 2008), *Gug^{03928}, Kdm2^{KG04325}, lid^{k06801}, nom^{EY064946}*, *chn^{02064}* and *lola^{00642}* (Bellen et al., 2011; 2004; Spradling et al., 1999), *Elongin-B^{EP3132}* (Rørth, 1996),*crp^{RAR46}* (Ashburner et al., 1999), *Alh^{r13}* (Lewis et al., 1980), *skd^{2}* (Kennison and Tamkun, 1988), *UAS-Sin3A-187* and *UAS-Sin3A-220* (Spain et al., 2010), *Df(2L)BSC184, Df(2L)BSC278, Df(3L)BSC389, Df(3R)BSC633, Df(3R)BSC478, Df(3R)BSC518* (Cook et al., 2012), *Df(2R)Exel7121* (Parks et al., 2004), *Df(2R)ED2076, Df(2R)ED2426* and *Df(3R)ED5331* (Ryder et al., 2007).

Antibodies Used in This Study

The following antibodies were used: anti-myosin heavy chain (1:500; gift of S. Abmayr), anti-β-galactosidase (1:1000; Abcam), rabbit anti-GFP (1:250; AbCam), mouse anti-GFP (1:500; Invitrogen), anti-dsRed (1:400, Clontech), anti-Krüppel (1:1000; gift of J. Reinitz), anti-Slou (1:200; (Cox et al., 2005)), anti-Sin3A (1:1000; gift of L. Pile), anti-β-PSintegrin (1:100, Developmental Studies Hybridoma Bank), anti-Alh (1:1000; (Bahri et al., 2001)), anti-Skd (1:5000; (Janody et al., 2003)), anti-crp (1:500; gift of M. Lehmann), anti-Chn (1:50; gift of E. Lai), anti-Elongin-B (1:50; Santa Cruz), and anti-Stripe A (1:200; gift of T. Volk).

in situ Hybridization

Probes for in situ hybridization were made using clones from the DGC collection (Stapleton et al., 2002). Selected clones were grown in 96-well plates with all

subsequent processing also performed in 96-well format. DNA was isolated using the Qiagen DirectPrep 96 miniprep kit and transferred to PCR plates. PCR using primers to vector sequences flanking the cDNA and phage promoter (sequences available upon request) were then used to create a linear substrate suitable for in vitro transcription (IVT). 5 µl of PCR product was used directly for an IVT reaction containing digoxygenin-labeled dUTP according to standard ISH probe labeling protocols (Tautz and Pfeifle 1989). IVT reactions were cleaned up using Qiagen MinElute 96-well PCR cleanup plates, resuspended in hybridization buffer, and stored at –20°C until use.

Hybridizations were performed using Millipore MADV N65 filter plates essentially as described (Tomancak et al. 2002). Hybridization was visualized using alkaline-phosphatase coupled anti-digoxygenin antibodies and direct observation using a dissecting microscope following transfer of each column into 48-well plates for better visualization. DNA templates were sequenced to confirm probe identity.

Primers Used in Quantitative PCR and ChIP

Primers used to amplify *Slou* were *forward*: GCATTTCGCTCCGATTACAT and *reverse:* GGAGACACTGCGGGATACTC. Primers used to amplify *mew* were *forward:* CAGAAAGACTGTGGCGATGA and *reverse:* CCTGATGGGCGATGAATAGT. Primers used to amplify *mys* were *forward:* TGGCGAGTGTCACTTGAGTC and *reverse:* CAACCACATTGGATGAATCG. Primers used to amplify *rp49* were *forward:* GGAGACACTGCGGGATACTC and *reverse:* GGCAAGGTATGTGCGTGATT.

Primers used to amplify the *Slou* ME were *forward*: TACCACGATAACTGCCTCCAC and *reverse:* GACGACTCACACGCTCAAGA. The control region used was at *CG18859* at were *forward:* TATCAAATCGCTCTGGCTTG and *reverse:* GAGTCCAAGAGCCTGGATGT.

SUPPLEMENTAL REFERENCES

Ashburner, M., Misra, S., Roote, J., Lewis, S.E., Blazej, R., Davis, T., Doyle, C., Galle, R., George, R., Harris, N., et al. (1999). An exploration of the sequence of a 2.9-Mb region of the genome of Drosophila melanogaster: the Adh region. Genetics *153*, 179–219.

Bahri, S.M., Chia, W., and Yang, X. (2001). The Drosophila homolog of human AF10/AF17 leukemia fusion genes (Dalf) encodes a zinc finger/leucine zipper nuclear

protein required in the nervous system for maintaining EVE expression and normal growth. Mech. Dev. *100*, 291–301.

Bellen, H.J., Levis, R.W., He, Y., Carlson, J.W., Evans-Holm, M., Bae, E., Kim, J., Metaxakis, A., Savakis, C., Schulze, K.L., et al. (2011). The Drosophila gene disruption project: progress using transposons with distinctive site specificities. Genetics *188*, 731–743.

Bellen, H.J., Levis, R.W., Liao, G., He, Y., Carlson, J.W., Tsang, G., Evans-Holm, M., Hiesinger, P.R., Schulze, K.L., Rubin, G.M., et al. (2004). The BDGP gene disruption project: single transposon insertions associated with 40% of Drosophila genes. Genetics *167*, 761–781.

Burgio, G., La Rocca, G., Sala, A., Arancio, W., Di Gesù, D., Collesano, M., Sperling, A.S., Armstrong, J.A., van Heeringen, S.J., Logie, C., et al. (2008). Genetic identification of a network of factors that functionally interact with the nucleosome remodeling ATPase ISWI. PLoS Genet *4*, e1000089.

Cook, R.K., Christensen, S.J., Deal, J.A., Coburn, R.A., Deal, M.E., Gresens, J.M., Kaufman, T.C., and Cook, K.R. (2012). The generation of chromosomal deletions to provide extensive coverage and subdivision of the Drosophila melanogaster genome. Genome Biol *13*, R21.

Cox, V.T., Beckett, K., and Baylies, M.K. (2005). Delivery of wingless to the ventral mesoderm by the developing central nervous system ensures proper patterning of individual slouch-positive muscle progenitors. Dev. Biol. *287*, 403–415.

Gomez-Skarmeta, J.L., Diez del Corral, R., la Calle-Mustienes, de, E., Ferré-Marcó, D., and Modolell, J. (1996). Araucan and caupolican, two members of the novel iroquois complex, encode homeoproteins that control proneural and vein-forming genes. Cell *85*, 95–105.

Halfon, M.S., Carmena, A., Gisselbrecht, S., Sackerson, C.M., Jiménez, F., Baylies, M.K., and Michelson, A.M. (2000). Ras pathway specificity is determined by the integration of multiple signal-activated and tissue-restricted transcription factors. Cell *103*, 63–74.

Janody, F., Martirosyan, Z., Benlali, A., and Treisman, J.E. (2003). Two subunits of the Drosophila mediator complex act together to control cell affinity. Development *130*, 3691–3701.

Kennison, J.A., and Tamkun, J.W. (1988). Dosage-dependent modifiers of polycomb and antennapedia mutations in Drosophila. Proc. Natl. Acad. Sci. U.S.a. *85*, 8136–8140.

Lewis, R.A., Kaufman, T.C., Denell, R.E., and Tallerico, P. (1980). Genetic Analysis of the Antennapedia Gene Complex (Ant-C) and Adjacent Chromosomal Regions of DROSOPHILA MELANOGASTER. I. Polytene Chromosome Segments 84b-D. Genetics *95*, 367–381.

Neufeld, T.P., Tang, A.H., and Rubin, G.M. (1998). A genetic screen to identify components of the sina signaling pathway in Drosophila eye development. Genetics

148, 277–286.

Nose, A., Isshiki, T., and Takeichi, M. (1998). Regional specification of muscle progenitors in Drosophila: the role of the msh homeobox gene. Development *125*, 215–223.

Parks, A.L., Cook, K.R., Belvin, M., Dompe, N.A., Fawcett, R., Huppert, K., Tan, L.R., Winter, C.G., Bogart, K.P., Deal, J.E., et al. (2004). Systematic generation of high-resolution deletion coverage of the Drosophila melanogaster genome. Nat Genet *36*, 288–292.

Rørth, P. (1996). A modular misexpression screen in Drosophila detecting tissue-specific phenotypes. Proc. Natl. Acad. Sci. U.S.A. *93*, 12418–12422.

Ryder, E., Ashburner, M., Bautista-Llacer, R., Drummond, J., Webster, J., Johnson, G., Morley, T., Chan, Y.S., Blows, F., Coulson, D., et al. (2007). The DrosDel deletion collection: a Drosophila genomewide chromosomal deficiency resource. Genetics *177*, 615–629.

Spradling, A.C., Stern, D., Beaton, A., Rhem, E.J., Laverty, T., Mozden, N., Misra, S., and Rubin, G.M. (1999). The Berkeley Drosophila Genome Project gene disruption project: Single P-element insertions mutating 25% of vital Drosophila genes. Genetics *153*, 135–177.

Tautz, D. and Pfeifle, C. (1989) A non-radioactive in situ hybridization method for the localization of specific RNAs in Drosophila embryos reveals translational control of the segmentation gene hunchback. Chromosoma. *98,* 81-5.